JOURNAL OF APPLIED ELECTROCHEMISTRY 7 (1977) 57–64

# *Investigation of hydrophobic porous electrodes. II. Pseudocapacitance changes during underpotential copper deposition*

J. McHARDY

*EIC Corporation, 55 Chapel Street, Newton, Mass. 02158, USA*

Received 22 March 1976

Differential capacitance measurements in 96% *o*-phosphoric acid at 160° C have been used to follow the underpotential deposition of copper on supported platinum in a porous electrode. At a potential in the range 0·2–0·3 V versus RHE the capacitance, $C$, increased as copper deposition proceeded and a plot of $C$ versus $t^{1/2}$ was linear during a substantial part of the deposition process. The slope $dC/dt^{1/2}$ was proportional to the copper concentration in solution, suggesting that the $Cu/Cu^{2+}$ pseudocapacitance reflected the quantity of copper deposited and that copper deposition was diffusion controlled. The effective diffusion coefficient estimated from the results was $10^{-7}$ cm$^2$ s$^{-1}$ – some 40 times smaller than the copper ion diffusion coefficient measured separately. At potentials of 0·4 V and above, capacitance measurements could not be used to follow copper deposition because the $Cu/Cu^{2+}$ pseudocapacitance decayed with time.

## 1. Introduction

Quantitative investigation of electrocatalysis at small metal particles ($\leqslant$ 100 Å diameter) has become possible only recently with the advent of supported electrocatalysts [1]. Platinum supported on carbon black can be prepared with a surface area in excess of 100 m$^2$ g$^{-1}$ (particles $<$ 30 Å diameter) but some degree of sintering tends to occur during subsequent testing, especially at the elevated temperatures characteristic of fuel cell operation [2]. *In situ* measurements of platinum surface area during electrocatalysis tests are thus desirable and copper deposition was examined as a possible basis for such measurements. (The more established technique of hydrogen deposition can be used only in fully flooded electrodes [3].) In the course of the work, some interesting observations were made concerning the time dependence of the $Cu/Cu^{2+}$ pseudocapacitance during underpotential deposition and these observations are the subject of the present note. A novel approach to platinum surface area determination emerged from the work and a procedure suitable for routine measurement is outlined in the Appendix.

## 2. Experimental

Tests were performed at 160° C in 96% phosphoric acid (made by concentrating Fisher Certified 85% *o*-phosphoric acid) which contained additions of cupric oxide. Gases, nitrogen and helium, were C.P. grade. Diffusion coefficients were measured at a Pt wire electrode by recording potentiostatic transients in the manner described by Klinedinst *et al.* [4]. The adsorption isotherm for copper on platinum was measured on a porous Pt disc by the multi-pulse potentiodynamic technique [5]. The disc was made by pressing 350 mg of 100 mesh Pt powder in an 0·75 inch diameter die at a pressure of 4000 psi and then sintering it at 1200° C for 15 min. Capacitance measurements were performed on specimens cut from a single sample of a PTFE-bonded porous electrode. The electrode contained approximately 4 mg cm$^{-2}$ of a 10% Pt/carbon black electrocatalyst on a carbon paper backing. Similar electrodes have been described previously [6]. Test specimens were 1·7 cm diameter discs from which an annular region of the catalyst layer had been scraped off the backing to leave 1 cm$^2$ of electrode material in the center. The specimens

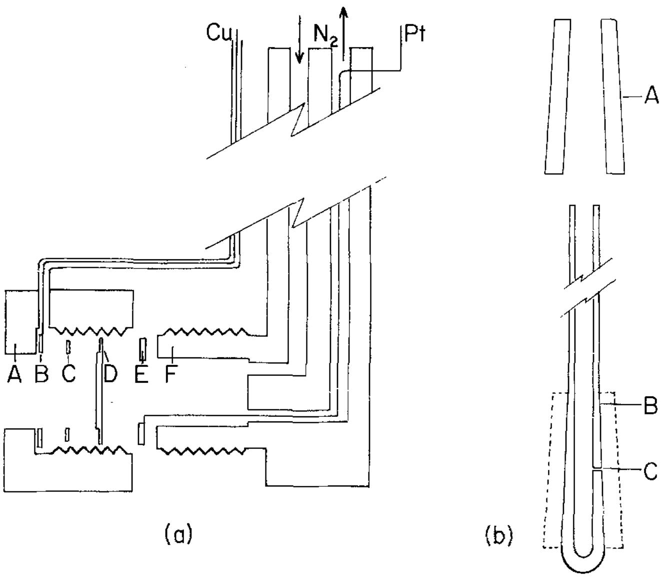

Fig. 1(a). Screw-cap electrode holder: A. PTFE cap; B. Cu ring; C. PTFE spacer; D. Electrode; E. Pt. ring; F. PTFE body.
Fig. 1(b). Reference electrode compartment: A. Female Ground Glass Joint, size 7/25 (Dotted line shows position during use); B. Male Ground Glass Joint, size 7/25; C. 0·5 mm Hole.

were tested in the screw-cap holder illustrated in Fig. 1(a). The thin copper ring incorporated in the holder was used as an a.c. reference electrode to minimize noise pickup. After immersion in the solution for a few minutes, the copper ring settled down to a constant potential in the vicinity of 0·18 V versus RHE (the reversible hydrogen electrode) and actually proved quite reliable as a d.c. reference electrode. Potentials were monitored continuously on a digital voltmeter (Data Technology Model 350) against a bubbling $H_2$/platinum black reference electrode which occupied the compartment shown in Fig. 1(b). The reference compartment was immersed in the test cell close to the working electrode and ionic contact was maintained by capillary action between the two ground glass surfaces. The arrangement minimized access to the reference electrode by copper ions and no poisoning was detected even in the longest experiments (~ 100 h).

Differential capacitance measurements were performed by the low frequency a.c. impedance technique described previously [7]. The improved signal-to-noise ratio brought about by using a low resistance reference electrode (the copper ring) instead of a Luggin capillary allowed measurements to be made with a smaller voltage amplitude than before. Unless otherwise stated, a test signal of ± 6 mV at 1 Hz was employed for the impedance measurements.

Platinum surface areas were calibrated at 25° C by the hydrogen deposition method in 1 M $H_2SO_4$ solution [3].

## 3. Results

### 3.1 *Diffusion measurements*

The wire electrode used for the diffusion experiments was 0·038 cm in diameter and 1·80 cm in length. After potentiostatting the electrode at 0·90 V in helium saturated solution for 5 min, the potential was stepped to 0·00 V and the current transient recorded. Tests were repeated until three successive runs yielded identical $i$–$t$ curves. A replot of the data against $t^{-1/2}$ yielded straight lines typified by Fig. 2. The success of the technique depends upon the electrode reaction (copper deposition in the present case) being under pure diffusion control throughout the current transient. A potential below 0·00 V would ensure this condition but hydrogen evolution would interfere. To check the validity of data obtained at 0·00 V, the test was performed with two copper concen-

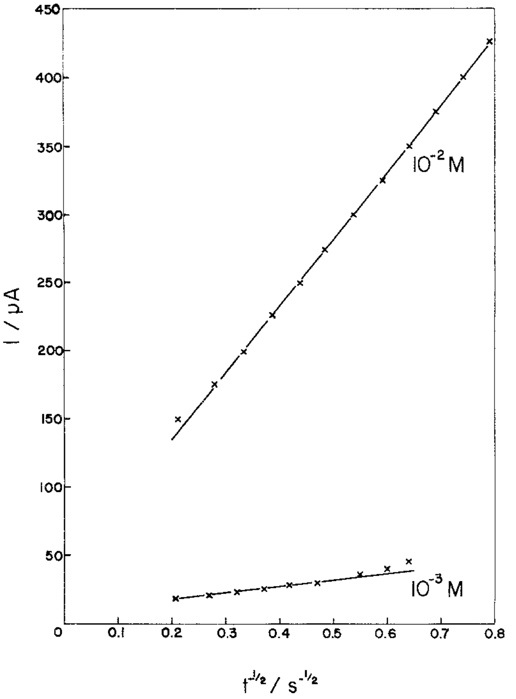

Fig. 2. Plots of current versus $(\text{time})^{-1/2}$ at a Pt wire electrode following a potential step from 0·90 to 0·00 V (160° C, 96% $H_3PO_4$).

trations. The diffusion coefficient, $D$, was calculated from the equation [4]

$$i = [nFA(D/\pi)^{1/2}]\, ct^{-1/2} \qquad (1)$$

where $A$ = geometric surface area; $n$ = number of electrons transferred during copper ion discharge (taken as 2); $c$ = copper concentration in solution; $t$ = time. The values of $D$ obtained from the data in Fig. 2 were $4{\cdot}4 \times 10^{-6}\ \text{cm}^2\,\text{s}^{-1}$ (lower curve) and $3{\cdot}8 \times 10^{-6}\ \text{cm}^2\,\text{s}^{-1}$ (upper curve). This agreement is within the experimental error and an average value of $4 \times 10^{-6}\ \text{cm}^2\,\text{s}^{-1}$ was adopted.

### 3.2. *Adsorption measurements*

Results of potentiodynamic sweep experiments on a porous Pt disc are summarized in Fig. 3. Each sweep was preceded by a 5 min step at 0·9 V and a similar step at a lower potential (designated '$E$' in the inset diagram). Four experiments were performed, with $E$ taking the values 0·15, 0·20, 0·25 and 0·3 V, respectively. The anodic charge associated with copper dissolution was estimated by graphical integration of the area above the dotted

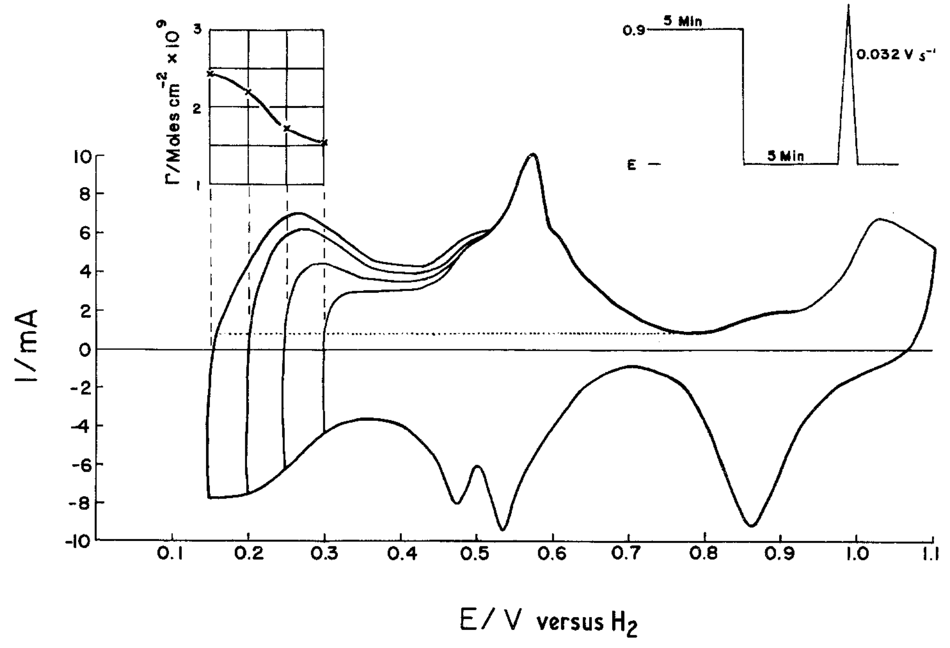

Fig. 3. Triangular voltage sweeps on a porous Pt disc produced by the inset potential program. Sweeps started at 0·15, 0·20, 0·25 and 0·30 V. The charges for Cu dissolution were integrated graphically, converted to moles of Cu $\text{cm}^{-2}$ of Pt and used to construct the inset adsorption isotherm (160° C; 96% $H_3PO_4$; $10^{-2}$ M $Cu^{2+}$).

line for each sweep. The resulting plot of equilibrium copper coverage versus potential is included in the diagram. Note that the plot goes through an inflection point in the interval between 0·2 and 0·3 V. The slope of the plot in this region is about $10^{-8}$ mol cm$^{-2}$ V$^{-1}$ which would correspond to a pseudocapacitance of the order of 2 mF cm$^{-2}$.

### 3.3 *Capacitance measurements*

Plots of capacitance versus potential for the porous Pt disc in three solutions appear in Fig. 4. The bottom curve represents just the double layer capacitance of the platinum and was taken from the previous paper [7]. For all practical purposes, the double layer capacitance can be neglected by comparison with the Cu/Cu$^{2+}$ pseudocapacitances in the upper two curves. In $10^{-2}$ M solution, the peak at low potentials falls short of the approximately 2 mF cm$^{-2}$ estimated from the adsorption isotherm. The estimate actually corresponds to a zero-frequency capacitance and the lower value measured at 1 Hz indicates that the Cu/Cu$^{2+}$ reaction is too slow to maintain equilibrium at this frequency. Raising the copper concentration to 3 x $10^{-2}$ M did increase the pseudocapacitance peak to about 2 mF cm$^{-2}$.

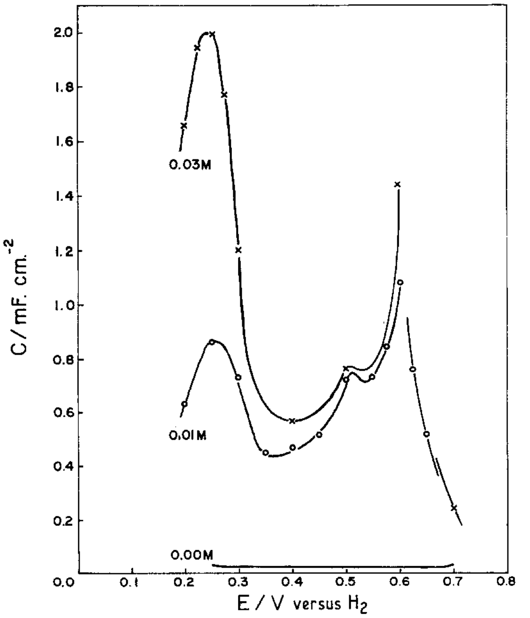

Fig. 4. Differential capacitance of a porous Pt disc as a function of electrode potential in 3 solutions. Each point was taken following a 10 min step at 0·90 V (160° C; 96% $H_3PO_4$).

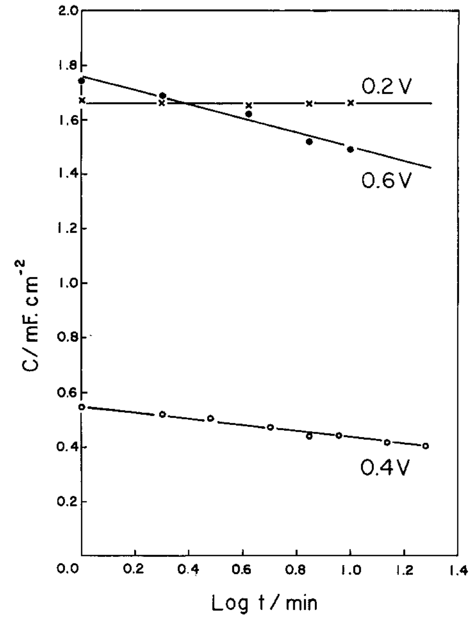

Fig. 5. Differential capacitance of a porous Pt disc as a function of log (time) at 3 potentials (160° C; 96% $H_3PO_4$; 3 X $10^{-2}$ M $Cu^{2+}$; Pretreated 10 min at 0·90 V).

Time dependences of the pseudocapacitance measured at various potentials on the Pt disc are illustrated in Fig. 5. At potentials of 0·3 V and below, the behaviour resembled that shown for 0·2 V, the capacitance being essentially constant. At potentials of 0·4 V and above, the capacitance decreased monotonically with time – apparently following a logarithmic relationship. Time dependences of the differential capacitance at 0·3 V measured on Pt/carbon porous electrodes are illustrated in Fig. 6. The two plots represent tests performed on different specimens in $10^{-2}$ M and 3 x $10^{-2}$ M Cu$^{2+}$ solutions. Over a substantial part of each plot, the capacitances increased linearly with $t^{1/2}$. The slope of the plots, $dC/dt^{1/2}$, were 1·9 x $10^{-2}$ F s$^{-1/2}$ and 6·0 x $10^{-2}$ F s$^{-1/2}$, respectively. In view of probable variations from one specimen to another, the ratio of these two slopes agrees very well with the 1:3 ratio of the two copper concentrations. A further test was performed in acid saturated with Cu$^{2+}$ ions (approximately $10^{-1}$ M) but capacitances could not be measured fast enough to 'catch' the linear $t^{1/2}$ region. The capacitance levelled off at $t^{1/2} \leqslant 8\ s^{1/2}$ which was about a third of the corresponding value in 3 x $10^{-2}$ M solution and a tenth of the value in $10^{-2}$ M solution. A reasonable conclusion

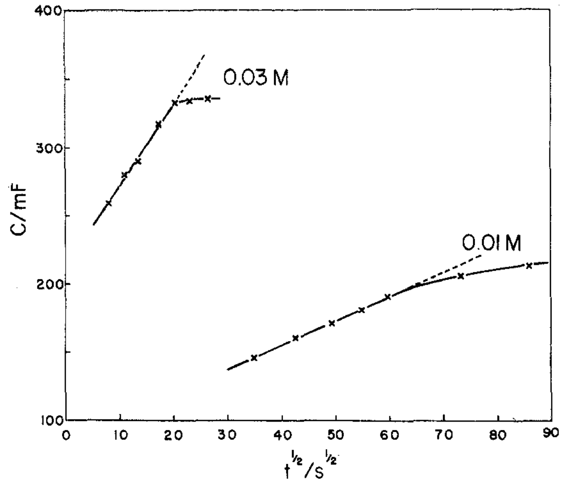

Fig. 6. Differential capacitance of 1 cm$^2$ porous Pt/carbon black electrodes at 0·30 V as a function of (time)$^{1/2}$ in 2 solutions (160° C; 86% $H_3PO_4$; Pretreated 10 min at 0·90 V).

to be drawn from these results is that the slope $dC/dt^{1/2}$ is directly proportional to $c$, the copper ion concentration in solution, i.e.,

$$dC/dt^{1/2} = Kc \tag{2}$$

where K is an empirical constant.

## 4. Discussion

Integrating Equation 2 yields:

$$C - C_0 = Kct^{1/2} \tag{3}$$

where $C_0$ is the value of $C$ at $t = 0$. Equation 3 may be compared with an equation for semi-infinite linear diffusion:

$$q = [2nFA(D/\pi)^{1/2}]\, ct^{1/2} \tag{4}$$

which is the integrated form of Equation 1. The similarity between Equations 3 and 4 suggests that $C$ is a linear function of $q$ – the quantity of copper deposited – and that the deposition process is diffusion controlled. An examination of these two inferences will occupy the next few paragraphs.

### 4.1 *Diffusion in porous electrodes*

Since we are concerned only with diffusion in the liquid phase, the model used by Austin and Lerner [8] is appropriate. According to this model, the pores are so highly interlinked that the concentration of the reactant at any point is determined by a single parameter: the penetration depth into the electrode. Diffusion into the electrode thus takes place linearly but the effective diffusion coefficient, $D^*$, is smaller than that for true linear diffusion, $D$. To arrive at the relationship between $D$ and $D^*$, consider an electrode with $N$ pores cm$^{-2}$, each of radius, $r$, and tortuosity, $\tau$. The ratio of $D^*$ to $D$ is equal to the cross-sectional area available for diffusion per cm$^2$ of electrode, i.e., $N\pi r^2$. The pore volume per cm$^3$ is $N\pi r^2\tau$ but for a fully flooded electrode, this is equal to the porosity $\epsilon$. Consequently, the term $N\pi r^2$ may be replaced by $\epsilon/\tau$ and hence the relationship between true and effective diffusion coefficients is [9]:

$$D^* = D\epsilon/\tau. \tag{5}$$

In order to apply Equation 5 to an electrode that is only partially filled with electrolyte, the porosity, $\epsilon$, must be replaced by the 'wetted porosity', $\epsilon'$, and in a simple model, the ratio of $\epsilon'$ to $\epsilon$ would be just the fraction of the pore volume occupied by electrolyte.

### 4.2 *Interpretation of capacitance measurements*

In the absence of dissolved copper, the capacitance of a Pt/carbon black electrode is essentially just the double layer capacitance of the carbon and at 0·3 V, the value for a typical electrode is about 0·1 F cm$^{-2}$. Inspection of Fig. 6 reveals that the capacitance, $C_0$, obtained by extrapolating a $t^{1/2}$ plot to zero-time, is a function of copper concentration. In $10^{-2}$ M solution $C_0$ is close to the value expected for the double layer capacitance but in $3 \times 10^{-2}$ M solution, $C_0$ is significantly larger. The difference can be explained in terms of finite copper coverages at zero time (i.e., when the potential was switched from 0·9 to 0·3 V). Electrolyte contained in the pores will be depleted of copper as soon as the potential is lowered, providing a small but uniform coverage on the platinum. (Deposition on carbon was not detected at the potentials employed in these experiments). This zero-time coverage would increase with the nominal concentration of copper in solution and make a correspondingly larger contribution to the measured capacitance. The concentration profile immediately after switching to 0·3 V will thus be a step function where the copper concentration drops to zero at the surface of the electrode. As equilibrium coverage is reached on Pt particles close to the front of the electrode, the concentration 'step' will propagate into the electrode and the pseudocapacitance will increase in proportion to the depth of penetration. As long as this ideal situation is maintained, the diffusion will follow semi-infinite linear behaviour with an effective diffusion coefficient, $D^*$, given by Equation 5.

From Fig. 6, it is possible to determine the value of $t^{1/2}$ at which equilibrium copper coverage would occur if the entire diffusion process took place according to Equation 4. The quantity of copper which must enter the electrode to provide equilibrium coverage can be calculated from a knowledge of the Pt surface area and the Cu adsorption isotherm (Fig. 3). For the 1 cm$^2$ electrodes in Fig. 6, the calculated quantity of copper for equilibrium coverage at 0·3 V was $2{\cdot}3 \times 10^{-7}$ mol. The values of $t^{1/2}$ at which the linear plots extrapolate to $C_\infty$ (the steady state capacitance) were 73 s$^{1/2}$ for $10^{-2}$ M solution and 21 s$^{1/2}$ for $3 \times 10^{-2}$ M solution. Substituting these values in Equation 4 yields estimates for $D^*$ of $0{\cdot}8 \times 10^{-7}$ and $1{\cdot}0 \times 10^{-7}$ cm$^2$ s$^{-1}$, respectively. Thus, $D^*$ is some 40 times smaller than the true diffusion coefficient measured above. Substituting this ratio of $D$ to $D^*$ in Equation 5 we obtain the result:

$$\frac{\epsilon'}{\tau} = \frac{1}{40} \qquad (6)$$

Now the tortuosity, $\tau$, approaches unity for a highly porous medium [9] and therefore, the 'wetted porosity', $\epsilon'$, of the electrodes can be only a few %. By contrast the electrodes normally took up a volume of phosphoric acid equal to about half the total porosity and the value of $\epsilon'$ expected from a simple model would be about 40%.

Evidently, the distribution of electrolyte in a hydrophobic porous electrode is more complex than predicted from the currently accepted 'flooded agglomerate' model [10] and considerable refinement of the model is needed.

## 5. Conclusions

(1) At potentials of 0·3 V and below, capacitance measurements can be used to follow the underpotential deposition of Cu on Pt in a porous electrode.

(2) Underpotential deposition in the system investigated was a diffusion controlled process.

(3) During most of the deposition, the process obeyed the semi-infinite linear diffusion equation with an effective diffusion coefficient some 40 times smaller than the true diffusion coefficient.

(4) At potentials of 0·4 V and above, capacitance measurements could not be used to follow copper deposition because the Cu/Cu$^{2+}$ pseudocapacitance decayed with time. This phenomenon warrants further study.

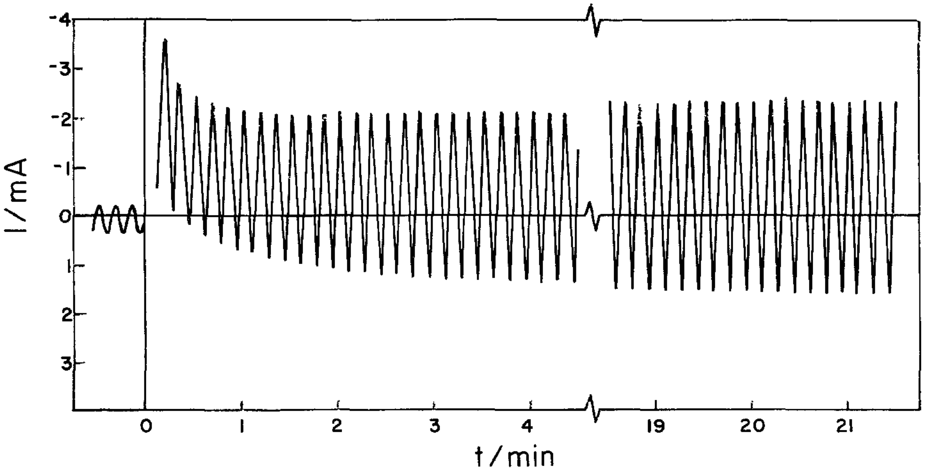

Fig. 1'. Typical recorder trace of current versus time at a 1 cm$^2$ porous Pt/carbon black electrode produced by a potential step from 0·90 to 0·24 V (160° C; 96% $H_3PO_4$; $3 \times 10^{-2}$ M $Cu^{2+}$; a.c. signal ± 5 mV at 0·1 Hz).

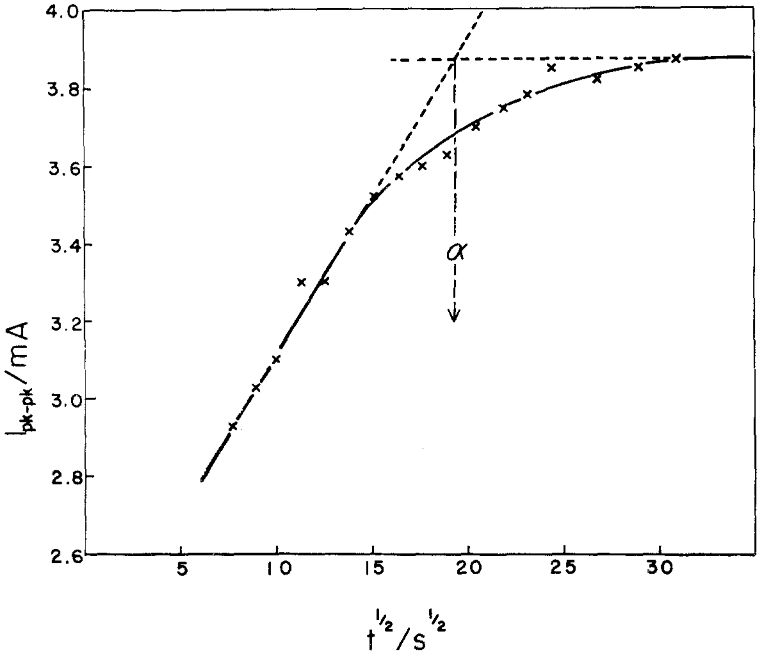

Fig. 2′. a.c. amplitude in Fig. 1′ as a function of (time)$^{1/2}$. The parameter α is obtained by extrapolating the linear region to the steady state value.

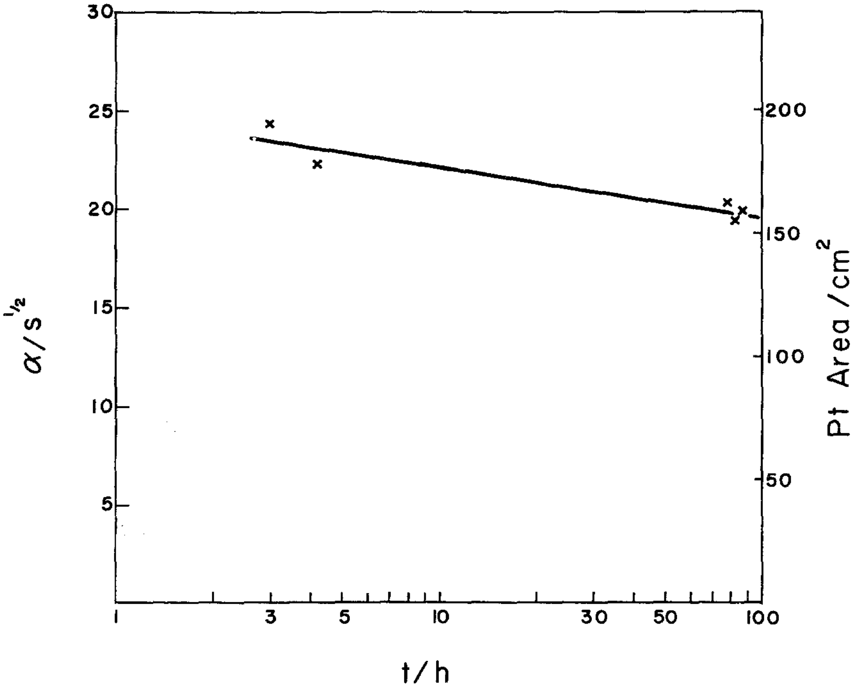

Fig. 3′. Pt surface area in a Pt/carbon black electrode in terms of the parameter α as a function of time under test. Right-hand ordinate labelled on the basis of post-test calibration (160° C; 96% $H_3PO_4$; $3 \times 10^{-2}$ M $Cu^{2+}$; 0·24 V).

## Appendix

*Procedure for measuring Pt surface area in porous electrodes*

Experimental conditions were chosen as follows: 160° C; 96% $H_3PO_4 + 3 \times 10^{-2}$ M $Cu^{2+}$; a.c. signal ± 5 mV at 0·1 Hz; d.c. potential held at 0·90 V for at least 10 min before switching to the test potential of 0·24 V. The current was recorded on a strip chart recorder (Varian model G-14) as the p.d. across a precision 1 Ω resistor in series with the counter electrode. Portions of a typical current versus time chart appear in Fig. 1′.

The small amplitude sine wave at $t < 0$ corresponded to the double layer capacitance of the electrode at 0·90 V. A cathodic d.c. current was superimposed on the a.c. current at $t > 0$ but it rapidly decayed to a low constant value and did not interfere with measurement of the a.c. amplitude.

The a.c. amplitude was then plotted versus $t^{1/2}$ as shown in Fig. 2′. Extrapolating the linear part of the plot to the steady state value gave the parameter $\alpha$ and over a series of tests, this parameter decreased as shown in Fig. 3′.

To a reasonable approximation, the a.c. amplitude in this test may be taken as a measure of the electrode capacitance [11] (the error at 0·1 Hz is less than 5%) and consequently, $\alpha$ measures the quantity of copper deposited in the electrode. Fig. 3′ thus shows Pt surface area decreases with time. After test, the final Pt surface area was determined in 1 M $H_2SO_4$ by H adsorption [3]. The scale on the right-hand side of Fig. 3′ is based on this calibration point. In practice it may not be necessary to obtain a calibration point for every electrode but many factors will influence the relation between $\alpha$ and Pt area ($Cu^{2+}$ concentration; electrode structure; temperature; etc.) so a new calibration would be advisable whenever test conditions alter.

## Acknowledgement

The application of underpotential copper deposition to the measurement of platinum surface area in a fuel cell electrode was originally suggested by R. Breault of the Power Systems Division, United Technologies Corporation.

## References

[1] K. Kinoshita and P. Stonehart, *Electrochim. Acta* **20** (1975) 101.
[2] J. A. Bett, K. Kinoshita and P. Stonehart, *J. Catalysis* **35** (1974) 307.
[3] D. Ferrier, K. Kinoshita, J. McHardy and P. Stonehart, *J. Electroanal. Chem.* **61** (1975) 233.
[4] K. Klinedinst, J. A. S. Bett, J. MacDonald and P. Stonehart, *ibid* **57** (1974) 281.
[5] S. Gilman, *J. Chem. Phys.* **68** (1964) 2098.
[6] H. R. Kunz and G. A. Gruver, *J. Electrochem. Soc.* **122** (1975) 1279.
[7] J. McHardy, J. Baris and P. Stonehart, *J. Appl. Electrochem.* **6** (1976) 371.
[8] L. G. Austin and H. Lerner, *Electrochim. Acta* **9** (1964) 1469.
[9] P. C. Carman, 'Flow of Gases Through Porous Media,' Academic Press, New York (1956).
[10] J. Giner and C. Hunter, *J. Electrochem. Soc.* **116** (1969) 1124.
[11] L. Ramaley and C. G. Enke, *ibid* **112** (1965) 943.